M. A. Brovelli & M. Cannata

DIGITAL TERRAIN MODEL RECONSTRUCTION IN URBAN AREAS FROM AIRBORNE LASER SCANNING DATA: THE METHOD AND THE EXAMPLE OF THE TOWN OF PAVIA (NORTHERN ITALY)

M. A. Brovelli , M. Cannata

Polytechnic of Milano - Campus Como - Via Valleggio, 12- 22100 Como (Italy)
Tel:+39-02-23997517, Fax:+39-02-23997519
maria@ipmtf4.topo.polimi.it,   maxi@geomatica.ing.unico.it

Commission II, WG II /2

KEY WORDS: Lidar, Tychonov regularization, urban areas, DTM extraction

ABSTRACT:

Lidar techniques represent a new and fruitful approach in the determination of digital surface models. One of the goals in processing this data is to set up filtering methods allowing to automatically extract the ground and the features (buildings, vegetation,…) superimposed on the terrain itself. In our work the emphasis is posed on the first topic. The method implemented took advantage of the use of spline functions regularized by means of Tychonov functional in a least squares approach. The DSM pixels have been classified in order to previously detect the edges of the non terrain features; the second step is the identification of all the pixels corresponding to the ground, by means of a region growing algorithm and its correction. By a new interpolation only made from the ground pixel we finally get to the digital terrain model. In the paper the processing methodology is discussed and a first large real example is presented.

1. INTRODUCTION

The new techniques based on laser scanning observations allow to obtain, in the measurement area, a very detailed surface digital model (DSM), with the possibility of interpolating the data on grids also characterised by 1m x 1m resolution.

The observations, interesting because of the high informative content particularly in the frame of geographic 3D features modelling, must be processed in order to automatically extract from the raw data, both the digital terrain model (DTM) and the shape of the man-made features superimposed on it. The latter last from the geometric point of view can be modelled by points, lines and polygons (or collections of them) which are not coherent with the surrounding terrain model.

The proposed and implemented algorithms to treat polygonal surface are completely different from the ones which allow to single out point and linear entities.

Indeed, in the second case (point and line), the entities detection is based essentially on the following hypotheses:

- the digital terrain model is a regular surface which does not present remarkable discontinuities;
- the point heights are independent of far points, but are correlated to points in the same surroundings.

The second hypothesis allows us to build up statistical tests based on localised procedures (comparison between the observed value and the value predicted in the point by using the surrounding measurements) while the first allows to choose, as interpolating models, simple functions (e.g. polynomial models). Work has been done following the previous hypotheses and the results on a real example (detection of long distance power lines) give a good result.

As is easy to guess, the method fails in cases of polygonal surfaces detection. To this aim we have then proposed a completely different approach explained in the next paragraphs.

2. THE METHOD

2.1 Overview

The method proposed can be summarised in the following steps:

- interpolation of raw data to obtain a regular grid, taking into account the problem of the regions with no observations (bicubic splines interpolation with hybrid norm Tychonov regularization);
- edges detection, based on two considerations:
  1. the features edges are 'outliers' corresponding to sharp rise of the surface;
  2. the residuals between the raw and interpolated elevation are positive inside the objects and negative outside them.

  As the information from these is spatially incorrelated, we have at first classified the edges by using a threshold for the gradient and then we have thinned the edges taking into account only the pixels corresponding to the objects.

- Region growing algorithm application to determine the convex surface inside the edges. Once we have detected the edge of all the features present, we classify all the pixels inside them. At first we have simply applied a region growing algorithm. However the procedure fails in some cases like for instance the saw-toothed roofs of industrial sheds or other eccentric roofs. Moreover in case like the ones of isolated trees the procedure (due to the oscillation of the bicubic splines) leads sometimes to overestimate

their dimension or to introduce new non-existent slivers of features.

- Localised procedure to correct the misclassified pixels. The procedure is tuned up by two correcting parameters. Several experiments have set up the optimal parameters forareas with different feature content (open field, vegetation, buildings,...).

- Removal from the observations of those corresponding to non ground elements.

- Interpolation of the ground observations by means of the procedure seen at point 1. In this case, taking into account the hypothesis of regularity of the digital terrain model, we have applied to obtain the final grid a bilinear spline interpolation with slope minimisation.

In the next we explain in detail the more interesting points.

2.2 Spline Functions and Tychonov Regularization

The starting step consists in modelling the raw observations by using spline functions and the least squares approach. To this aim the observation equations read:

$$h_0\left(\underline{t}_m\right) = \sum_{lk} a_{lk} s_\Delta{}^g\left(\underline{t}_m - \underline{\tau}_{lk}\right) + v_m \qquad (1)$$

where $h_0\left(\underline{t}_m\right)$ are the observed altimetric values (m=1,N);

[l,k] are the knot grid indices;

g describes the spline function type
(g=1 bilinear splines, g=3 bicubic splines)

Δ is the grid step;

$s_{\Delta_{lk}}\left(\underline{t}\right) = s_\Delta\left(\underline{t} - \underline{\tau}_{lk}\right)$ is a function which determining a translation of the compact support which centres the spline at the generic grid knot $\underline{\tau}_{lk}$.

The function has been given by the Cartesian product of the monodimensional splines.

In the linear case we have:

$$s^{(1)}(\underline{t}) = s^{(1)}(x,y) = \begin{cases} \varphi_{11} & \begin{cases} x \in [-2\Delta,0] \\ y \in [-2\Delta,0] \end{cases} \\ \varphi_{12} & \begin{cases} x \in [-2\Delta,0] \\ y \in [0,2\Delta] \end{cases} \\ \varphi_{21} & \begin{cases} x \in [0,2\Delta] \\ y \in [-2\Delta,0] \end{cases} \\ \varphi_{22} & \begin{cases} x \in [0,2\Delta] \\ y \in [0,2\Delta] \end{cases} \end{cases} \qquad (2)$$

where:

$$\varphi_{11} = \frac{(2\Delta+x)(2\Delta+y)}{16\Delta^4}$$

$$\varphi_{12} = \frac{(2\Delta+x)(2\Delta-y)}{16\Delta^4}$$

$$\varphi_{21} = \frac{(2\Delta-x)(2\Delta+y)}{16\Delta^4} \qquad (3)$$

$$\varphi_{22} = \frac{(2\Delta-x)(4\Delta-y)}{16\Delta^4}$$

Instead, the bicubic spline reads:

$$s^{(3)}(\underline{t}) = s^{(3)}(x,y) = \begin{cases} \varphi_{33}(x,y) & \begin{cases} x \in [0,2\Delta] \\ y \in [0,2\Delta] \end{cases} \\ \varphi_{43}(x,y) & \begin{cases} x \in [2\Delta,4\Delta] \\ y \in [0,2\Delta] \end{cases} \\ \varphi_{34}(x,y) & \begin{cases} x \in [0,2\Delta] \\ y \in [2\Delta,4\Delta] \end{cases} \\ \varphi_{44}(x,y) & \begin{cases} x \in [2\Delta,4\Delta] \\ y \in [2\Delta,4\Delta] \end{cases} \end{cases} \qquad (4)$$

where:

$$\varphi_{33} = \frac{(4\Delta-x)^3 - 4(2\Delta-x)^3}{96\Delta^4} \frac{(4\Delta-y)^3 - 4(2\Delta-y)^3}{96\Delta^4}$$

$$\varphi_{43} = \frac{(4\Delta-x)^3}{96\Delta^4} \frac{(4\Delta-y)^3 - 4(2\Delta-y)^3}{96\Delta^4}$$

$$\varphi_{34} = \frac{(4\Delta-x)^3 - 4(2\Delta-x)^3}{96\Delta^4} \frac{(4\Delta-y)^3}{96\Delta^4} \qquad (5)$$

$$\varphi_{44} = \frac{(4\Delta-x)^3}{96\Delta^4} \frac{(4\Delta-y)^3}{96\Delta^4}$$

In order to avoid as much as possible cells empty of data, the grid resolution has to be set by taking into account the minimum distance of each observation with respect to the others. A possible choice can be the means of the minimum values.

However, it has to be remarked that, even if Δ is of the same magnitude as the mean minimum distances between the observations, due to the irregularity of the data distribution, cells without data still can remain.

Moreover if the size of an empty region is such that some unknown parameter doesn't appear in any equation, a rank deficiency results.

This problem is related both to the grid step and to the degree of the spline function: in same cases, for instance, if we model the data by means of bilinear splines a singularity in the least squares normal matrix arouses, while if we use bicubic ones the problem has overcame.

A more general approach to face singularity consists in performing an hybrid norm interpolation: we add, in the least squares principle, a condition assuring the solution uniqueness even in case of lack of data.

Starting from

$$\underline{Y}_0 = A\underline{a} + \underline{v} \tag{6}$$

in which:

$$
\begin{cases}
\underline{Y_0} = [\,...\, h_0\left(\underline{t}_m\right)\,...]^t \\
\underline{a} = [\,...\, a_{lk}\,...]^t \\
\\
A = \begin{bmatrix} ... & ... & ... & ... \\ ... & s_\Delta{}^g\left(\underline{t}_m - \underline{\tau}_{lk}\right) & ... & ... \\ ... & ... & ... & ... \\ ... & ... & ... & ... \end{bmatrix}
\end{cases} \tag{7}
$$

The regularised estimator of the $\underline{a}$ coefficients is obtained by minimising a linear function composed by two non negative parts:

$$Min\,\Psi(\underline{a}) = Min\left\{ \left|\underline{Y}_0 - \hat{Y}\right|^2 + \lambda K(\underline{a}) \right\} = \Psi(\underline{a}) \tag{8}$$

where:

$\left|\underline{Y}_0 - \hat{y}\right|$ = usual least square minimising functional; $K(\underline{a})$ = regularising positive function:

$K(\underline{a}) \to \infty$ for $\underline{a} \to \infty$;
λ = regularising parameter.

Usually, for the sake of simplicity, we take as $K(\underline{a})$ a quadratic function: $K(\underline{a}) = \underline{a}^t \mathbf{K} \underline{a}$ ($\mathbf{K} = \mathbf{K}^t, \mathbf{K} \geq 0$). In this case the estimation equations are linear.

By applying the generalised least square principle, we obtain the following normal system:

$$(A^t A + \lambda \mathbf{K})\hat{\underline{a}} = D_\lambda \hat{\underline{a}} = A^t \underline{Y}_0 \tag{9}$$

where $\mathbf{K}$ has to meet the condition $\mathrm{rank}(A^t A + \lambda\mathbf{K}) = n$ in order to guarantee the solution uniqueness.

The regularising function to be chosen depends on the terrain morphology. Let us assume, as usual, the terrain surface as a function $h(\underline{t})$.

In case there are not sharp slope or curvatures changes, we respectively assume that:

$$\int \left[h^2 + \left|\nabla h\right|^2 \right] dt < \infty \tag{10}$$

or

$$\int \left[h^2 + \left|\Delta h\right|^2 \right] dt < \infty \tag{11}$$

Thus, as Tychonov regularisation function, we take into account:

$$K(h) = \int \left|\nabla h\right|^2 dt < \infty \tag{12}$$

$$K(h) = \int \left|\Delta h\right|^2 dt < \infty \tag{13}$$

respectively in order to control the slope (12) the curvature (13). Just to have an idea of the behaviour of the interpolating surface in case of lack of data in Fig. 1 the two solution corresponding to (12) and (13) in one dimension have been shown. The first solution is more rough, but allows to slope changes, while the second one leads spurious oscillation in case of sharp slope changes. Recalling the two different degree spline functions previously mentioned, we decide to associate respectively (12) and (13) to $h(t)$ modelled by means of bilinear and bicubic splines.
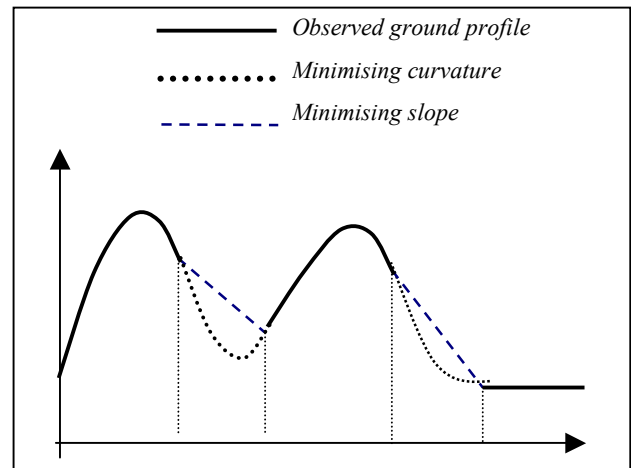
Figure 1. Behaviour of the regularisation functions (12) and (13)

The regularisation functions have to be discretized to be applied to our problem.

$\mathbf{K}$ is a matrix (n x n) containing the first or second order derivatives of the $h(\underline{t})$ surface in each grid knot.
In case of bilinear splines we have:

$$\mathrm{h}\left(\underline{\tau}_{lk}\right) \equiv a_{lk} \tag{14}$$

from which we obtain the discretized form of the gradient:

$$\left|\nabla \mathrm{h}\left(\underline{\tau}_{lk}\right)\right|^2 \cong \left(\frac{a_{l+1,k} - a_{l-1,k}}{2\Delta}\right)^2 + \left(\frac{a_{l,k+1} - a_{l,k-1}}{2\Delta}\right)^2 \tag{15}$$

45

and thus the *K(a)* functional:

$$K(\underline{a}) \cong \frac{1}{4} \sum_{lk} \left\{ (a_{l+1,k} - a_{l-1,k})^2 + (a_{l,k+1} - a_{l,k-1})^2 \right\} \qquad (16)$$

Analogously in case of bicubic splines we get:

$$h(\underline{\tau}_{lk}) \equiv h_{lk} = \frac{4}{9} a_{lk} + \frac{1}{9} (a_{l+1,k} + a_{l-1,k} + a_{l,k+1} + a_{l,k-1}) + \qquad (17)$$
$$+ \frac{1}{36} (a_{l+1,k+1} + a_{l-1,k+1} + a_{l-1,k-1} + a_{l+1,k-1}),$$

$$(\Delta h)_{lk} = \frac{1}{\Delta^2} \left\{ h_{l+1,k} + h_{l-1,k} + h_{l,k+1} + h_{l,k-1} - 4h_{l,k} \right\} \qquad (18)$$

and finally:

$$K(\underline{a}) = \sum_{l,k} (\Delta h)_{l,k}^2 \, \Delta^2 . \qquad (19)$$

3. THE EXAMPLE

3.1 The Original Data

The procedures and algorithms implemented have been applied on a LIDAR data set acquired in November 1999 on the town of Pavia and its immediate neighbourhood with Toposys sensor. The flight height was around 850 meters (a part from two halved height cross strips). The point density was roughly 5 points per square meter and a one-meter grid was computed and delivered. The total data set covers an area corresponding to around 3248 x 7245 m^2. The characteristics of the data, corresponding to the last pulse observations, are summarised in Table 1.

As it is clear from the characteristics shown in Table 1, the area is almost flat and this is an advantage in our investigation.

The method developed is based on least square approach: we must therefore subdivide data into tiles and process them separately to avoid a possible storage exhaustion due to the dimension of the normal matrix. Tiles have been bordered by adding suitable strip of data at each side to prevent or at least reduce the border distortion in the interpolating procedure.

UTM South-North coordinates	5'002'097.000 - 5'005'345.000
UTM East-West coordinates	508'000.000 - 515'245.000
Grid resolution South-North	1 m
Grid resolution East -West	1m
Cells with data	23'531'760
Cell without data	4'200'537
Maximum height	245.44 m
Minimum height	25.64 m
Mean height	68.30 m
Standard deviation	9.97 m

Table 1. Statistics of the original data

In this way tiles are partially overlapped and we to have a double solution for each border observation. The mean of the two interpolated heights weighted taking into account the distance between the datum and the edges of the tiles at which it belongs will use as input in the final computation of the DTM.

3.2 Feature Edge Detection

Starting from the two hypotheses already mentioned in paragraph 2.1, we need to compute the difference between the original and the interpolated values and the gradient in each observation point.

Thus the first step has consisted in interpolating the observation by means of bicubic splines and the minimum curvature regularisation functional seen in the paragraph 2.2.

The regularising parameter has been set, after various tests, equal to 1. An example of the interpolated surface is shown in figure 2: the surface represents a smoothing image of the DSM.
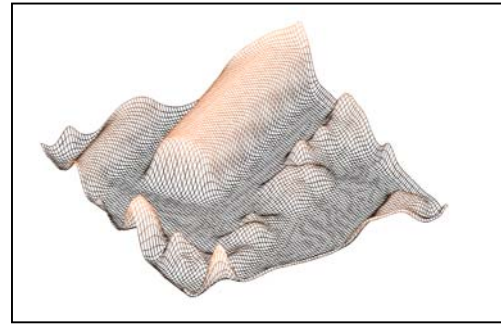
Figure 2. Bicubic spline surface with Tychonov regularisation (extract from the global DSM)

The gradient at each point has been computed applying to the interpolated values (in order to avoid the presence of gross errors) a 3x3 mask:

$$G(j,k) = \left\{ [G_H(j,k)]^2 + [G_V(j,k)]^2 \right\}^{1/2} \qquad (20)$$

where:

$$G_H = \frac{1}{2+\sqrt{2}} \begin{bmatrix} 1 & 0 & -1 \\ \sqrt{2} & 0 & -\sqrt{2} \\ 1 & 0 & -1 \end{bmatrix}, \; G_V = \frac{1}{2+\sqrt{2}} \begin{bmatrix} -1 & -\sqrt{2} & -1 \\ 0 & 0 & 0 \\ 1 & \sqrt{2} & 1 \end{bmatrix}$$

The pixels with gradient greater than 50 have been classified as edge pixels (Fig. 3a)

The residuals between the observed and the interpolated values are positive inside the features and negative outside them: this criterion has been used to thin the edges (Fig. 3b).
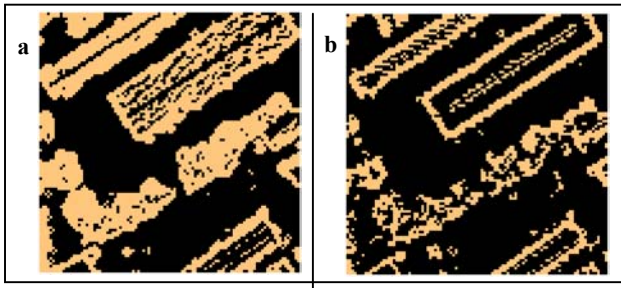
Figure 3. Edge detection from gradient (a) and adding the residual sign information (b) (extract from the global DSM)

3.3 Edges Filling Up

Once detected the edges of the objects, we have to fill up them. The proposed procedure consists in two steps. The first is a region growing algorithm: a moving 3x3 mask is centred at each point classified as object: each pixel in the mask whose value is greater or equals the central value is classified as object. The algorithm fails in case of eccentric roofs with pitches at different heights (Fig. 4). Moreover another case of misclassification occurs when isolated height discontinuities (e.g.: trees) are present: to maintain the minimum curvature the interpolating surface gives rise to spurious oscillations. The classification based on positive residuals and high gradient modulus recognizes as edge also the ground close to the peak and the region growing algorithm fills up a region greater than the actual feature dimension (Fig. 5).
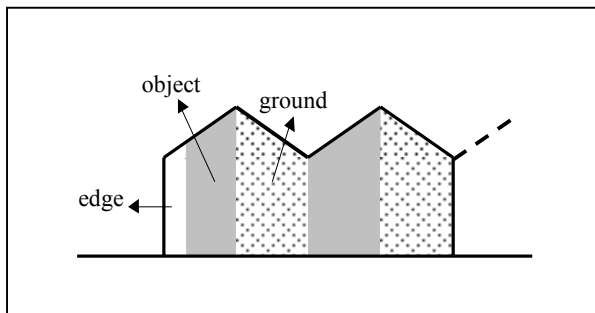
Figure 4. Edge detection and region growing in case of eccentric roof

To correct the classification, the whole tile has been subdivided into subtiles: in each of them a bilinear surface has been computed only from the heights of the ground pixels: all the pixels classified as objects and closer to the surface less than a threshold are reclassified as ground pixels; all the pixels classified as ground and further than the second threshold from the surface are taken into account as object pixels.

The dimension of the subtiles ('dim') and the two thresholds ('ground height', 'house height') have been tuned up tile by tile taking into account the morphology and landuse of the zones.
We have recognized within the 36 tiles three kind of areas:

- 9 urban areas with: 'dim'= 50 m, 'house height' = 1.5 m, 'ground height'=1.5 m,
- 10 rural areas with: 'dim'= 90 m, 'house height' = 1.5 m, 'ground height'=1.5 m
- 10 industrial areas. These last have been the more complex to model because of the presence of the saw-toothed roofs

of the sheds have push us up in choosing time to time the suitable parameters.
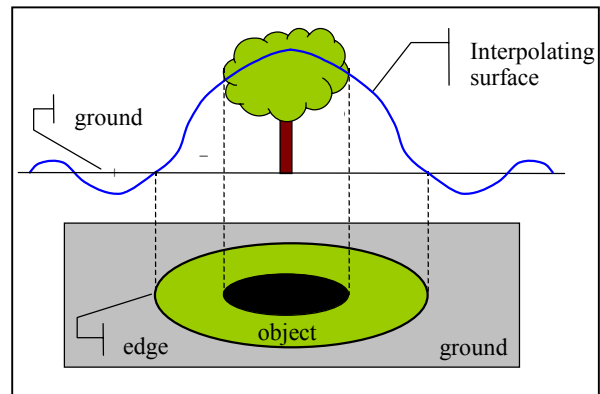
Figure 5. Edge detection and region growing in case of isolated peak

3.4 DTM Computation

First of all we analyze the heterogeneity within the overlapping zones. An example of heterogeneity is shown in Fig. 6. Obviously a systematic relation between the difference in the parameters used and the classification heterogeneity percentage exists. Anyway by our algorithm the classification errors lead to an over estimation of the pixels classified as objects.
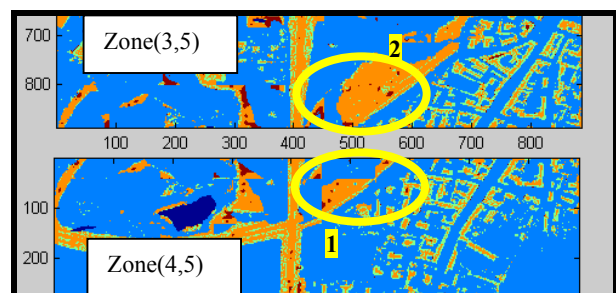
Figure 6. Classification heterogeneity in two overlapping zones.

Thus, in order to avoid distortion in the DTM, the pixels classified at least one as object, have been left out of the final computation: the high observation resolution and the availability of the algorithm to manage the lack of data allows us to pick out only the more probable ground pixels.

The final DTM computation has been performed by interpolate the ground observations by means of bilinear splines and slope minimisation. The regularising λ parameter has been choosen equal to 1 . The global DTM has been obtained patching the partial ones of each tile. In the pixels belonging to the overlapping regions the mean height weighted referring to the distance of the pixel from the edge of the tile, has been computed.

3.5 Comparisons and Conclusions

The output DTM covers the same area and has a resolution of 10 x 10 m^2. To verify the correctness of the final result acomparison with two independent data set has been performed:

- the heights of the levelling point network of the Pavia map at scale 1:500, determined within the altimetric tolerance of 0.25 m;
- the heights of 17 points used as control points for the photogrammetric survey done contemporary to the laser scanning.

In the first case, after the removal of no corresponding points (for instance in our DTM features like bridges are not considered as part of the terrain, on the contrary in levelling data the heights are measured on them) we remained with 687 points. The statistics of the differences between the two heights sets (mean=-0,01 m and rms=0,66 m) show a good agreement between them (see Fig. 7). The highest differences are mostly attributable to points on the river banks and can not be considered mistake, as our method, representing the "natural DTM', does not model the retaining walls of the riverside.
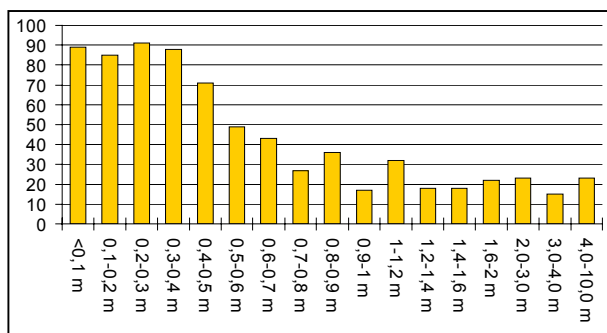
Figure 7. Histogram of differences between lidar and levelling heights (source: Pavia technical map)

The agreement between LIDAR and photogrammetric control points, in which GPS levelling have been performed is even better. In fact, as shown in Table 1, the difference are greater than 1 meter only in the cases of points 4 and 13.

The first point is on an elevated road (Fig. 8), while our DTM reproduces the natural ground behaviour; the same happens at point 13, which is on the embankment (Fig. 9).

Concluding we feel that our methodology is performing very well, though some refinements are still necessary.

point #	LIDAR heights (m)	Differences (m)
1	73.2617	0.088
2	71.9653	0.314
3	66.5686	0.152
4	60.3848	6.436
5	60.4784	0.077
6	62.4465	0.256
7	77.7738	0.131
8	74.9569	0.451
9	79.6286	0.891
10	74.0923	0.325
11	77.3464	0.363
12	68.7543	0.160
13	59.5656	1.608
14	60.3506	0.672
15	73.2104	0.350
16	72.5288	0.927
17	78.3855	-0.120

Table 1. Differences between LIDAR and GPS heights at the photogrammetric control points

Figure 8. Point on a elevated road in which the differences between GPS and LIDAR heights are higher than 1 m.

Figure 9. Point on an embankment in which the differences between GPS and LIDAR heights are higher than 1 m.

REFERENCES

K. Kraus, N. Pfeifer. 1998. Determination of terrain models in wooded areas with airbone laser scanner data, *ISPRS Journal of Photogrammetry & Remote Sensing*, 53 (4), 245 – 261.

M. A. Brovelli, M. Reguzzoni, F. Sansò, G. Venuti 2001. *Procedure diricostruzione del modello digitale del terreno da dati laser scanning,* Bollettino SIFET.

M. A. Brovelli, M. Reguzzoni, F. Sansò, G. Venuti 2001. Modelli matematici del terreno per mezzo di interpolatori a spline, Bollettino SIFET.

M. Ziegler, A. Wimmer, R. Wack 2001. DTM Generation by Means of Airbone Laser Scanning – An Advanced Method for ForestedAreas. *In 5th Conference on Optical 3-D Mesurement Techniques*, Vienna.